INSTITUTE OF PHYSICS PUBLISHING JOURNAL OF PHYSICS: CONDENSED MATTER

J. Phys.: Condens. Matter **18** (2006) 9335–9357 doi:10.1088/0953-8984/18/41/003

Isotropic-to-nematic transition in liquid-crystalline heteropolymers: I. Formalism and main-chain liquid-crystalline polymers

Paul P F Wessels[1] **and Bela M Mulder**

FOM Institute for Atomic and Molecular Physics (AMOLF), Kruislaan 407, 1098 SJ Amsterdam, The Netherlands

E-mail: mulder@amolf.nl

Received 19 January 2006, in final form 28 June 2006
Published 29 September 2006
Online at stacks.iop.org/JPhysCM/18/9335

Abstract

We formulate a density functional approach for arbitrarily branched liquid-crystalline (LC) heteropolymers consisting of elongated rigid rods coupled through elastic joints. The theory exactly accounts for the energetic and entropic single-chain effects, whereas the interchain excluded volume effects are treated within the Onsager approximation. We apply the theory to finite-length main-chain LC polymers composed of rigid mesogens coupled by flexible spacers of finite length, modelled initially as chains of thin rods. The theory then allows an easy passage to the wormlike chain limit for the spacers. Employing a bifurcation analysis we analytically obtain the stability boundaries of the isotropic phase towards the nematic liquid crystalline phase, as a function of the relative size of the mesogens with respect to the spacers and the spacer flexibility. From the same analysis we also obtain the distribution of the incipient nematic ordering at the spinodal density as a function of position along the chain, including the end-effects.

1. Introduction

A generic mesogen, or liquid-crystal (LC) forming molecule, is an elongated molecule with a relatively stiff molecular core. If such molecules are incorporated as subunits in a polymeric compound, one can obtain a substance that couples the optical properties of an LC (birefringence, field orientability) with the mechanical and processing properties of polymers. Over the years these so-called LC polymers have received widespread attention, also due to their potential for applications [1–6].

There are two main classes of LC polymers; those where the mesogenic subunits are incorporated within a linear polymeric structure are called main-chain LC polymers, and those

[1] Present address: ABN-AMRO Corporate Research, Amsterdam, The Netherlands.

0953-8984/06/419335+23$30.00

which have the mesogenic units attached to the side of a polymer backbone are called side-chain LC polymers. An essential concept in LC polymeric systems is the insertion of 'spacer' groups to spatially separate the mesogens. This was first realized by Finkelmann *et al* [7–9] for side-chain LC polymers, but later also applied to main-chain LC polymers. These spacers are usually aliphatic chains, which, being rather flexible, act to decouple the rigid mesogenic groups from the backbone polymer (side-chain LC polymers) or from each other (main-chain LC polymers). The spacers basically allow the mesogenic groups to order orientationally relatively unhindered, while at the same time the polymer chain as a whole is not frustrated greatly in exploring different conformations and thus maximizing its entropy. This means that in LC polymeric phases the spacers (and polymeric backbone, if present) will be necessarily less ordered than the mesogens.

Through the pioneering work by Onsager [10], Flory [11], and Maier and Saupe [12], we possess a thorough theoretical understanding of LC behaviour in simple rodlike molecules. The task of modelling LC polymers, however, is a much more challenging one. The individual polymers have many degrees of freedom and are statistical systems in their own right, whose behaviour, even in the absence of interactions with other molecules, involves both entropic and energetic aspects. The latter are due to the steric interactions between neighbouring components, which translate into a (temperature dependent) resistance to bending. As it turns out, the degree of flexibility of the polymers is a key ingredient in describing phase behaviour of LC polymers.

The seminal theories aimed at modelling main-chain LC polymers are due to Khokhlov and Semenov [13, 14] and Warner and co-workers [15, 16]. These works focused strongly on the molecular flexibility, by treating the polymers as wormlike chains, i.e. continuous space curves with a resistance to bending distributed homogeneously along their length.

However, real main-chain LC polymers are heterostructures, consisting of components with different spatial dimensions and different degrees of flexibility. Several lattice model approaches have been proposed in which these types of details were incorporated [17–21]. A typical artifact of these approaches is the appearance of nematic–nematic transition between phases with a weak and a strong degree of order.

Two rather similar off-lattice approaches to treating a main-chain LC polymer composed of rigid rods coupled by elastic spacers were developed by Yurasova and co-workers (YC) [22–24] and by Wang and Warner (WW) [25]. Both these theories employ a Maier–Saupe-like mean-field approach and assume the spacers to be wormlike chains. They differ in their treatment of the statistics of the spacers, YC opting for the so-called spherical approximation [26], whilst WW employ the arguably more powerful spheroidal wavefunction expansion [15]. In both cases, however, only the average degree of order of the spacers is determined and the chains are implicitly infinite in length, so neither local variations in ordering along the polymer nor end-effects due to finite polymer length are addressed.

In principle, more detailed information could come from simulations. However, simulations of genuine LC polymers (with hundreds to thousands of repeating units) are beyond present-day computational capabilities. On the one hand, a number of simulations have been reported which focus on larger systems and longer timescales consisting of structurally simple LC polymers interacting via coarse-grained 'simple' potentials [27–30]. A typical example we would like to mention is the work of Lyulin *et al* [29], where main-chain LC polymers are modelled as repeating units of Gay-Berne mesogens with five to eight Lennard-Jones atoms acting as connecting spacers. They were able to simulate 64 polymers with the degree of polymerization being 10 for about 10 ns, and find both an isotropic and a nematic phase. On the other hand, there are a few simulations using more realistic atomic-level potentials, but in these the systems were necessarily smaller and the timescales correspondingly shorter [31, 32].

Our aim is to set up a general framework for modelling LC polymer behaviour that is (i) detailed enough to discuss features caused by the local connectivity of the components, (ii) allows for structural heterogeneity and (iii) still simple enough to allow the extraction of the phase behaviour as function of a limited number of parameters. In this way we hope to address some of the limitations of the theoretical and computational approaches discussed above and provide a tractable tool for rational prediction of LC polymer properties.

Although most LC polymers are thermotropic, with main exceptions being biopolymers like DNA or bio-aggregates like viruses, we nevertheless choose to develop a density functional theory based on the polymeric components being hard rigid rods. The arguments for this choice are twofold. Firstly, anisotropic short range repulsions are the major determinant of fluid state structure and form the basis of the modern theory of simple liquids. Additional energetic interactions can, if required, always be added to a hard core system in a perturbative manner. Secondly, as we will treat the excluded volume interactions in the Onsager approximation, we will obtain a theory that is formally equivalent to a Maier–Saupe-like mean-field theory for softer potentials, if one neglects the effects of compressibility. This equivalence can be used to map the results of the purely lyotropic case pursued here to the thermotropic case.

Our model LC polymers are composed of elongated hard rigid cylindrical rods. Different types of rods are distinguished on the basis of their dimensions (length and width). These rods can be linked to each other and with each link we associate a bending potential which can depend on the type of rods being linked. A major novelty of our approach is that we allow multiple links to any rod, thus creating complex topologies. As it turns out we are still able to take into account all single polymer degrees of freedom *exactly* even for arbitrary branched polymers, as long as there are no closed loops in the structure. The resultant class of 'treelike' polymers encompasses both side-chain LC polymers as well as LC dendrimers. An interesting precursor to our work, unknown to us at the time of writing, is the paper by Stott and Petschek [33], who consider both random and regular three-functional dendrimers formed from identical LC moieties connected by orientational springs, mimicking the presence of spacer chains. Their formalism already captures the essence of the generalization to branched structures, albeit in a less generic framework and without treating the spacer groups on an equal footing with the other chain components.

We have already presented a restricted version of the theory applied to linear homopolymers in [34], while a specific application to side-chain LC polymers was briefly addressed in [35]. The purpose of the present work is to present the general theory and the details of its application to a generic main-chain LC polymer composed of two components, mesogens and spacers, and a side-chain LC polymer with three components (backbone, side-group spacers and mesogens). For length reasons, however, we relegate the discussion of the latter part to a companion paper [36]. Our focus is on analytical results regarding the location of phase boundaries and the distribution of order along the polymers. To this end we employ the tools of bifurcation analysis extensively.

The outline of the paper is as follows. In section 2, we first set up the model and the appropriate statistical mechanical formalism. We then deduce the self-consistency equations describing the stationary phases and discuss the conditions for phase equilibrium. We show that the problem complexity is dramatically reduced by projecting on the subsets of segments of a specific type. We then turn to a generic form of the bifurcation equations, again stressing the notion of 'type averaging'. In section 3 we take on the application to a model main-chain LC polymer, discussing the model parameters and how to take the wormlike chain limit for the spacers. We go on to present the bifurcation analysis and its results. We close with a discussion and outlook.

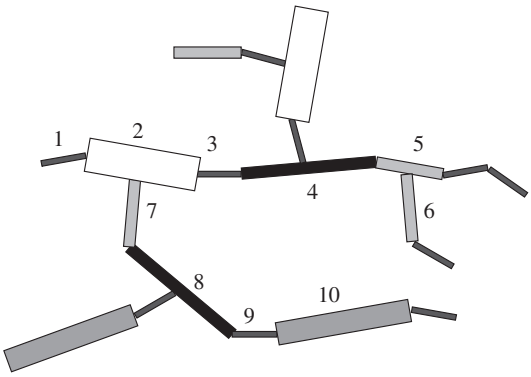

Figure 1. A branched heterochain of rodlike segments. The explicit example of a segment labelling is added to show that, in the case of branched chains, segments with non-consecutive labels may still be nearest neighbours (like 2 and 7).

2. General LC heteropolymers

2.1. Model and formalism

2.1.1. Free energy functional and stationarity equation. The system we consider is a fluid of N identical (possibly) branched polymer chains in a volume V. Each chain is composed of M rigid cylindrically symmetric rodlike segments of R different types. The different types are distinguished by a label τ with $\tau \in \{1, \ldots, R\}$. A segment of type τ has a length l_τ and a diameter d_τ, where it is assumed that $l_\tau \gg d_\tau$. Each individual segment is labelled by an index m with $m \in \{1, \ldots, M\}$. To indicate that a given segment is of a certain type we will use the convenient rather than mathematically precise notation $m \in \tau$. If two segments m and m' are linked in the polymer, they become *neighbours*, which we express by the notation (m, m'). Any segment may link to more than two neighbouring segments, thus allowing arbitrary branched molecular structures, but we explicitly *exclude* the occurrence of closed loops of segments. The reason for the latter constraint will be discussed in section 2.1.2. The orientation of a segment is described by a unit vector $\hat{\boldsymbol{\omega}}_m$ pointing along its symmetry axis. The configuration $\boldsymbol{\xi}$ of a single polymer is specified by the position $\mathbf{R}$ of its centre of mass and its conformation $\boldsymbol{\Omega} = (\hat{\boldsymbol{\omega}}_1, \ldots, \hat{\boldsymbol{\omega}}_M)$, being the orientations of all segments. A schematic example of the type of branched heteropolymer we treat is given in figure 1.

The method of choice for dealing with order–disorder phenomena in classical liquids is density functional theory (DFT), which states that (i) the free energy can be formulated as a functional of the single-molecule (=chain) configuration distribution function $\rho^{(1)}(\boldsymbol{\xi})$ and (ii) the equilibrium phase can be determined from minimizing this functional [37]. The specific choice of approximate density functional we adopt here is a second virial, or Onsager, approximation at the level of the chains [34],

$$\beta\mathcal{F}\left[\rho^{(1)}\right] = \int \mathrm{d}\boldsymbol{\xi}\, \rho^{(1)}(\boldsymbol{\xi}) \left[\log\left(\mathcal{V}_\mathrm{T}\rho^{(1)}(\boldsymbol{\xi})\right) - 1\right] + \beta \int \mathrm{d}\boldsymbol{\xi}\, \rho^{(1)}(\boldsymbol{\xi}) U(\boldsymbol{\xi}) - \tfrac{1}{2} \int\int \mathrm{d}\boldsymbol{\xi}\, \mathrm{d}\boldsymbol{\xi}'\, \rho^{(1)}(\boldsymbol{\xi})\rho^{(1)}(\boldsymbol{\xi}')\Phi(\boldsymbol{\xi}, \boldsymbol{\xi}'), \tag{1}$$

where $\mathcal{V}_\mathrm{T}$ is the so-called thermal volume, being the product of the relevant de Broglie wavelengths, and $\beta = 1/k_\mathrm{B}T$ with k_B Boltzmann's constant and T the temperature. The two successive non-ideal terms in this free energy represent the internal energy of the chains

due to the bending potential U and an entropic interaction term due to the excluded volume interactions between the segments which is mediated by Φ, the chain–chain Mayer function. The integrals are over all configuration space, $\int \mathrm{d}\boldsymbol{\xi} = \int \mathrm{d}\mathbf{R}\,\mathrm{d}\boldsymbol{\Omega} = \int \mathrm{d}\mathbf{R} \prod_m \mathrm{d}\hat{\boldsymbol{\omega}}_m$, and $\rho^{(1)}$ is normalized to the number of particles, $\int \mathrm{d}\boldsymbol{\xi}\, \rho^{(1)}(\boldsymbol{\xi}) = N$. In this paper we only consider spatially homogeneous phases and therefore set $\rho^{(1)}(\boldsymbol{\xi}) = \rho f(\boldsymbol{\Omega})$, with $\rho = N/V$ the chain number density and $f(\boldsymbol{\Omega})$ the conformational distribution function of the whole chain (CDF). Necessarily, the CDF has the following normalization: $\int \mathrm{d}\boldsymbol{\Omega}\, f(\boldsymbol{\Omega}) = 1$.

We assume that the internal energy of the chain is entirely due to the bending potential operative between each linked pair of segments along the chain, hence

$$U(\boldsymbol{\Omega}) = \sum_{m,m'}^{(m,m')} u_{m,m'}(\hat{\boldsymbol{\omega}}_m \cdot \hat{\boldsymbol{\omega}}_{m'}). \tag{2}$$

where the summation is over all segments m and m' in the chain which are nearest neighbours (notation: (m, m')). We do not specify the exact form of $u_{m,m'}$ at this point, but point out that it may depend on the types of segments involved. Global rotational symmetry dictates its dependence on the orientations of the two linked segments through the inner product $\hat{\boldsymbol{\omega}}_m \cdot \hat{\boldsymbol{\omega}}_{m'} = \cos\theta_{m,m'}$. Note that the internal energy of a chain only depends on its conformation $\boldsymbol{\Omega}$ and not on its position $\mathbf{R}$. Note that the chosen form of the internal energy does not take into account the potential interactions due to overlap between segments other than nearest neighbours (which are effectively precluded from overlapping by the bending potential), so that the chains are allowed to intersect themselves.

As our chains are composed of hard, impenetrable, rods, the pair potential v is infinity when two chains overlap at any location and zero when they do not. The chain–chain Mayer function thus is

$$\Phi_{\mathrm{M}}(\boldsymbol{\xi}, \boldsymbol{\xi}') \equiv \exp(-\beta v(\boldsymbol{\xi}, \boldsymbol{\xi}')) - 1 = \begin{cases} -1 & \text{if overlap} \\ 0 & \text{if no overlap.} \end{cases} \tag{3}$$

Furthermore, realizing that the Mayer function is translationally invariant and as we are only considering homogeneous phases, we can define the so-called excluded volume of two chains

$$\mathcal{E}(\boldsymbol{\Omega}, \boldsymbol{\Omega}') = -\int \mathrm{d}(\mathbf{R} - \mathbf{R}')\, \Phi_{\mathrm{M}}(\mathbf{R} - \mathbf{R}', \boldsymbol{\Omega}, \boldsymbol{\Omega}'). \tag{4}$$

The excluded volume of two chains with arbitrary conformations, however, is too complicated to calculate. We therefore approximate the chain–chain excluded volume with the sum over all segment–segment excluded volumes

$$\mathcal{E}(\boldsymbol{\Omega}, \boldsymbol{\Omega}') = \sum_{m,m'} e_{m,m'}(\hat{\boldsymbol{\omega}}_m \cdot \hat{\boldsymbol{\omega}}_{m'}), \tag{5}$$

which for sufficiently elongated rods in fact is the first term in a systematic expansion of the chain–chain excluded volume (see [34] for details and a justification of this approximation). The segment–segment excluded volume depends on the type of segments involved and the planar angle γ between them and is taken to be equal to the asymptotic form due to Onsager

$$e_{m,m'}(\hat{\boldsymbol{\omega}}_m \cdot \hat{\boldsymbol{\omega}}_{m'}) = e_{\tau,\tau'}(\hat{\boldsymbol{\omega}}_m \cdot \hat{\boldsymbol{\omega}}_{m'}) = l_\tau l_{\tau'}(d_\tau + d_{\tau'})|\sin\gamma(\hat{\boldsymbol{\omega}}_m \cdot \hat{\boldsymbol{\omega}}_{m'})|, \tag{6}$$

where $m \in \tau$ and $m' \in \tau'$.

Given the definitions (2) and (5), we can perform the spatial integrations in equation (1) to obtain the free-energy functional per particle

$$\frac{\beta\mathcal{F}[f]}{N} = \log(\rho\mathcal{V}_{\mathrm{T}}) + \int \mathrm{d}\boldsymbol{\Omega}\, f(\boldsymbol{\Omega})\left[\log f(\boldsymbol{\Omega}) - 1\right] + \beta \int \mathrm{d}\boldsymbol{\Omega}\, f(\boldsymbol{\Omega}) U(\boldsymbol{\Omega}) + \tfrac{1}{2}\rho \int \mathrm{d}\boldsymbol{\Omega}\,\mathrm{d}\boldsymbol{\Omega}'\, f(\boldsymbol{\Omega}) f(\boldsymbol{\Omega}') \mathcal{E}(\boldsymbol{\Omega}, \boldsymbol{\Omega}'). \tag{7}$$

In thermodynamic equilibrium, the free energy is at a minimum and hence the functional must be stationary. We therefore consider the variation of equation (7) with respect to the CDF,

$$\frac{\delta}{\delta f(\mathbf{\Omega})}\frac{\beta\mathcal{F}}{N} - \beta\mu = 0 \tag{8}$$

with the chemical potential μ playing the role of Lagrange multiplier needed to enforce normalization. Eliminating μ from equation (8) yields the stationarity equation,

$$f(\mathbf{\Omega}) = Q^{-1}[f]\exp\left[-\beta U(\mathbf{\Omega}) - \rho\int \mathrm{d}\mathbf{\Omega}'\, f(\mathbf{\Omega}')\mathcal{E}(\mathbf{\Omega},\mathbf{\Omega}')\right] \tag{9}$$

in which Q is the normalization factor,

$$Q[f] = \int \mathrm{d}\mathbf{\Omega}\, \exp\left[-\beta U(\mathbf{\Omega}) - \rho\int \mathrm{d}\mathbf{\Omega}'\, f(\mathbf{\Omega}')\mathcal{E}(\mathbf{\Omega},\mathbf{\Omega}')\right]. \tag{10}$$

Because the chain–chain interaction term in our approximation, given by equation (5), only involves pair-wise segment–segment terms, we can obtain a reduced description in terms of single-segment orientational distribution function (ODF), which is defined as a 'projection' of the CDF onto a given segment,

$$f_m(\hat{\boldsymbol{\omega}}_m) = \int \prod_{k\neq m} \mathrm{d}\hat{\boldsymbol{\omega}}_k\, f(\mathbf{\Omega}). \tag{11}$$

With this definition we can rewrite equation (9) as a set of non-linear coupled self-consistency equations for the ODFs,

$$f_m(\hat{\boldsymbol{\omega}}_m) = Q^{-1}\int \prod_{k\neq m}\mathrm{d}\hat{\boldsymbol{\omega}}_k \times \prod_{k,k'}^{(k,k')} w_{k,k'}(\hat{\omega}_k,\hat{\omega}_{k'}) \prod_k \exp\left[-\rho\sum_{k'}\int \mathrm{d}\hat{\boldsymbol{\omega}}'\, e_{k,k'}(\hat{\boldsymbol{\omega}}_k,\hat{\boldsymbol{\omega}}')f_{k'}(\hat{\boldsymbol{\omega}}')\right]. \tag{12}$$

Here we have introduced the shorthand $w_{k,k'}(\hat{\boldsymbol{\omega}}_k,\hat{\boldsymbol{\omega}}_{k'}) = \exp[-\beta u_{k,k'}(\hat{\boldsymbol{\omega}}_k,\hat{\boldsymbol{\omega}}_{k'})]$ for the Boltzmann weight associated with the segment–segment bending interaction. The product $\prod_{k,k'}^{(k,k')}$ runs over all segments k and k' that are nearest neighbours along the chain, which we denote by the bracket (k,k').

To summarize, we mention that we have, either implicitly or explicitly, made three major approximations: (i) the Onsager or second virial approximation for the chain–chain interactions, (ii) multiple overlaps between two chains are not taken into account (a consequence of the approximation equation (5)) and (iii) the chains are not self-avoiding (equation (2)). Whilst it is beyond our present scope to fully discuss their validity, we point out that these approximations are commonly made and widely considered to include most of the essential physics, as least as far as bulk phase behaviour of polymer LCs is concerned [38, 39].

2.1.2. Local fields. At first sight the stationarity equation (12) appear to couple all the ODFs of the chain in a non-local fashion. At this point, however, our assumption on the topology of the chains, namely that, although allowed to be arbitrarily branched, they cannot contain any closed loops i.e. are *simply connected* [40], becomes crucial. This allows us to rewrite the stationarity equations in terms of *local* functions. These local functions are defined in a recursive manner and the structure of our chains guarantees that these recursions are both unique and finite. Specifically, for a given segment m we can write

$$f_m(\hat{\boldsymbol{\omega}}_m) = Q^{-1}\mathrm{e}^{-\beta\mathcal{H}_m(\hat{\boldsymbol{\omega}}_m)}\prod_{m'}^{(m,m')} q_{m,m'}(\hat{\boldsymbol{\omega}}_m) \tag{13}$$

where we have defined an effective (mean) field

$$\beta\mathcal{H}_m(\hat{\boldsymbol{\omega}}_m) = \rho \sum_{m'} \int \mathrm{d}\hat{\boldsymbol{\omega}}'\, e_{m,m'}(\hat{\boldsymbol{\omega}}_m, \hat{\boldsymbol{\omega}}')\, f_{m'}(\hat{\boldsymbol{\omega}}'), \tag{14}$$

which carries the effects due to the excluded volume interactions of the segment with other chains. The functions $q_{m,m'}$ code for the effects which are transmitted to the segment through its links to other parts of the chain on which it resides. They are defined through the following recursion relation:

$$q_{m,m'}(\hat{\boldsymbol{\omega}}_m) = \int \mathrm{d}\hat{\boldsymbol{\omega}}'_{m'}\, w_{m,m'}(\hat{\boldsymbol{\omega}}_m, \hat{\boldsymbol{\omega}}'_{m'}) \mathrm{e}^{-\beta\mathcal{H}_{m'}(\hat{\boldsymbol{\omega}}'_{m'})} \prod_{m''\neq m}^{(m',m'')} q_{m',m''}(\hat{\boldsymbol{\omega}}'_{m'}) \tag{15}$$

in terms of the same type of function now operating on the neighbours of segment m. One can follow these recursions along any branch of the polymer until one reaches a free end for which one defines $q_{m,\mathrm{end}} = 1$, which implies the absence of any net influence. A similar approach has often been applied in the theory of classical spin models on branching lattices (for a paradigmatic example see [41]).

The function $q_{m,m'}(\hat{\boldsymbol{\omega}}_m)$ is in fact the partition function of that part of the whole chain that is connected to m in the direction of m' under condition that the orientation $\hat{\boldsymbol{\omega}}_m$ of the 'root' segment m is kept fixed. Equivalently, $-\frac{1}{\beta}\log q_{m,m'}(\hat{\boldsymbol{\omega}}_m)$ is the potential of mean force imposed on segment m due to that same part of the whole chain. Note that the functions $q_{m,m'}$ are in general *not* symmetric in their labels; they depend specifically on the segment involved and on the direction from which their influence comes. The number of factors $q_{m,m'}$ acting on a segment depends on its connectivity within the chain. It is equal to 2 for a segment in a linear part of the chain, 1 for an end segment and 3 or more at a branching point. Finally, we point out that for a fixed set of effective external fields, equations (13) and (15) are an *exact* statement of the statistical mechanics of the isolated chains. It is in this sense that in our approach all *intra*chain effects, except for self-overlaps, are accounted for exactly. The major approximations involved enter through the definition of the effective field and its dependence on the *inter*chain interactions. It also shows that the statistical decoupling of different branches leading out from a single segment, introduced as an assumption in [33], is in fact an exact consequence of having only segment–segment interactions along the chains.

2.1.3. The isotropic and nematic phases. At low chain densities we expect the isotropic phase to be the stable one. In fact, it is not hard to see that the isotropic phase, for which $f_m(\hat{\boldsymbol{\omega}}_m) = 1/4\pi$, is a solution to equation (12) at any density. In that case the normalization constant, which is identical to the partition sum per chain, is equal to

$$Q_{\mathrm{iso}} = 4\pi \left(\prod_{k,k'}^{(k,k')} w^{(0)}_{k,k'} \right) \exp\left[-\frac{\rho}{4\pi} \sum_{k,k'} e^{(0)}_{k,k'} \right], \tag{16}$$

where $w^{(0)}_{k,k'}$ and $e^{(0)}_{k,k'}$ are the zeroth-order Legendre coefficients of $w_{k,k'}$ and $e_{k,k'}$ respectively (see equation (25)). At higher densities, we expect a uniaxially symmetric nematic phase to appear. In this case the ODFs are only a function of a single polar angle θ, between the segment axis $\hat{\boldsymbol{\omega}}_m$ and the preferred axis $\hat{\boldsymbol{n}}$ of the phase, and can therefore be expanded in a series of Legendre polynomials,

$$f_m(\theta_m) = \sum_{n=0}^{\infty} \frac{2n+1}{4\pi} a^{(n)}_m P_n(\cos\theta_m), \tag{17}$$

where of course

$$a^{(n)}_m = 2\pi \int_0^{\pi} \mathrm{d}\theta\, \sin\theta\, P_n(\cos\theta)\, f_m(\theta), \tag{18}$$

the factor 2π in front appearing due to the azimuthal integration ($\int \mathrm{d}\hat{\boldsymbol{\omega}} = \int_0^{\pi} \mathrm{d}\theta \, \sin\theta \int_0^{2\pi} \mathrm{d}\phi$). Furthermore, $a_m^{(0)} = 1$ for all m (because f_m is normalized and $P_0(\cos\theta) = 1$) and $a_m^{(2n+1)} = 0$ for all n as the uniaxial nematic phase is inversion symmetric. The coefficients $a_m^{(2)}$, $m = 1, \ldots, M$ are the primary order parameters, as these are the lowest order coefficients that differ between the isotropic and nematic phases.

The isotropic-to-nematic (I–N) transition generically is first order and will therefore involve a density jump of the system from ρ_{iso} to ρ_{nem}. These coexistence densities can be found by equating the pressure $\Pi_{\mathrm{iso}} = \Pi_{\mathrm{nem}}$ and chemical potential $\mu_{\mathrm{iso}} = \mu_{\mathrm{nem}}$ of the two phases, which both can be determined from the free energy

$$\beta\Pi = \rho^2 \frac{\partial\,(\beta\mathcal{F}/N)}{\partial\rho} \qquad \text{and} \qquad \beta\mu = \frac{\beta\mathcal{F}}{N} + \rho\frac{\partial\,(\beta\mathcal{F}/N)}{\partial\rho}. \tag{19}$$

In order to solve for the phase coexistence conditions, however, one needs to solve these equations in conjunction with the solution of the self-consistency equations equations (12) for the nematic phase. This is in general a challenging numerical task. In [34, 35], we have numerically computed ODFs in the nematic phase for linear homopolymers and side-chain polymers respectively. This is done by solving equations (13)–(15) by means of an iteration procedure along the lines of [42] and explained in more detail for linear homopolymers in [34]. In the following we will adopt a different approach, by performing a stability analysis of equation (12) starting from the isotropic phase. This locates the so-called spinodal or bifurcation point, the upper limit of stability of the isotropic phase, and a generally close upper bound on the transition density, and provides explicit information on the way the various parts of the polymer order. Moreover, it can be carried out fully analytically and yields additional insight into the factors that determine the transition.

Finally, it is sometimes reported that there exist various kinds of (uniaxial) nematic phases and first-order phase transitions between them in LC polymeric systems[2]. Nematic-to-nematic (N–N) transitions, being a transition between two phases of the same symmetry, require a 'van der Waals'-like loop in the pressure. Such a loop can be found by locating the spinodal points, $\rho^2\partial\Pi/\partial\rho = 0$. In our case we can compute the pressure explicitly from equations (7) and (19),

$$\begin{aligned}\beta\Pi &= \rho + \tfrac{1}{2}\rho^2 \int\int \mathrm{d}\boldsymbol{\Omega}\,\mathrm{d}\boldsymbol{\Omega}'\, f(\boldsymbol{\Omega}) f(\boldsymbol{\Omega}')\mathcal{E}(\boldsymbol{\Omega},\boldsymbol{\Omega}') \\ &= \rho + \tfrac{1}{2}\rho^2 \sum_{m,m'} \int\int \mathrm{d}\hat{\boldsymbol{\omega}}\,\mathrm{d}\hat{\boldsymbol{\omega}}'\, f_m(\hat{\boldsymbol{\omega}}) f_{m'}(\hat{\boldsymbol{\omega}}') e_{m,m'}(\hat{\boldsymbol{\omega}},\hat{\boldsymbol{\omega}}').\end{aligned} \tag{20}$$

This expression for the pressure shows that such spinodal points do not exist in this system, as the integral in equation (20) always has a positive value. Consequently, there are no (direct) N–N transitions for any type of LC polymers within our theory.

2.2. *Bifurcation analysis*

2.2.1. Bifurcation analysis at the segment level. In this section we proceed by studying equation (12) by means of a stability analysis of the isotropic phase. For low densities, the isotropic solution is the stable (and only) solution. Compressing the system, we arrive at the spinodal density at which the isotropic phase becomes unstable and a nematic appears. This density is also called the bifurcation density as at this point the low-symmetry solution, which is the nematic, branches off from the high-symmetry isotropic solution. For a first order transition, such as the I–N transitions discussed here, the bifurcation density yields an upper

[2] In [18–20] N–N transitions are described in main chain LC polymers, in [43, 44] for side-chain LC polymers and in [45] for dendrimers.

bound on the density at which the thermodynamic transition takes place [46, 47]. Close to the bifurcation point, the segment ODFs can be written as an isotropic distribution with an infinitesimal nematic perturbation,

$$f_m(\hat{\boldsymbol{\omega}}_m) = \frac{1}{4\pi} + \varepsilon f_m^{(1)}(\hat{\boldsymbol{\omega}}_m), \tag{21}$$

where $f_m^{(1)}$ has nematic symmetry (see equation (17)) and ε is an arbitrarily small parameter. Furthermore, we can assume without loss of generality that the $f_m^{(1)}$ are orthogonal with respect to the isotropic solution, i.e. $\int \mathrm{d}\hat{\boldsymbol{\omega}}\, f_m^{(1)}(\hat{\boldsymbol{\omega}}) = 0$.

Inserting the form equation (21) into the stationarity equation (12) we can expand both sides of the equation with respect to ε and collect terms of equal order. The zeroth-order contributions reduce to an identity by construction. To first order we obtain the *bifurcation equation*

$$f_m^{(1)}(\hat{\boldsymbol{\omega}}_m) = -\frac{\rho}{4\pi} \sum_k \int \prod_{j\neq m} \mathrm{d}\hat{\boldsymbol{\omega}}_j \prod_{j,j'}^{(j,j')} \frac{w_{j,j'}(\hat{\boldsymbol{\omega}}_j \cdot \hat{\boldsymbol{\omega}}_{j'})}{w_{j,j'}^{(0)}} \sum_{k'} \int \mathrm{d}\hat{\boldsymbol{\omega}}'\, e_{k,k'}(\hat{\boldsymbol{\omega}}_k \cdot \hat{\boldsymbol{\omega}}') f_{k'}^{(1)}(\hat{\boldsymbol{\omega}}') \tag{22}$$

which, in spite of its seemingly complex structure, can be seen as a linear eigenfunction problem with the density ρ being the eigenvalue and $f_m^{(1)}$ the eigenfunctions. Note that the rightmost sum (over k') in equation (22) is the amplitude to first order in ε of the effective field acting on segment k, since

$$\beta\mathcal{H}_k(\hat{\boldsymbol{\omega}}_k) = \frac{\rho}{4\pi} \sum_{k'} e_{k,k'}^{(0)} + \varepsilon\rho \sum_{k'} \int \mathrm{d}\hat{\boldsymbol{\omega}}'\, e_{k,k'}(\hat{\boldsymbol{\omega}}_k, \hat{\boldsymbol{\omega}}') f_{k'}^{(1)}(\hat{\boldsymbol{\omega}}'). \tag{23}$$

The first term in this expansion is a constant (independent of $\hat{\boldsymbol{\omega}}_k$) and hence irrelevant. Via the Boltzmann flexibility weights $w_{j,j'}$ this field is being 'passed on' along the chain until it reaches segment m, which is the 'target' segment appearing on the left side of the equation. We therefore define a path $\mathcal{P}_{k,m}$, which is the collection of all the pairs of nearest-neighbour segments that form the shortest connection between k and m. Again, due to the restricted topology of our chains, this path is uniquely defined. As an example, in figure 1, $\mathcal{P}_{4,8} = \{(4,3),(3,2),(2,7),(7,8)\}$. The Boltzmann flexibility weights $w_{j,j'}$ with $(j,j') \in \mathcal{P}_{k,m}$ are involved in passing on the field, whereas all others are not. Finally, there is another sum (over k) in equation (22), because all the segments in the chain experience the infinitesimal effective field, which eventually reaches segment m.

An important observation, which allows us to explicitly solve the bifurcation equations, is that the integration kernels $w_{k,k'}$ and $e_{k,k'}$ appearing in equation (22) both have uniaxial symmetry, so like the ODFs (see equation (17)) they can be expanded in Legendre polynomials,

$$\begin{bmatrix} w_{k,k'} \\ e_{k,k'} \end{bmatrix}(\cos\theta) = \sum_{n=0}^{\infty} \frac{2n+1}{4\pi} \begin{bmatrix} w_{k,k'}^{(n)} \\ e_{k,k'}^{(n)} \end{bmatrix} P_n(\cos\theta), \tag{24}$$

with coefficients

$$\begin{bmatrix} w_{k,k'}^{(n)} \\ e_{k,k'}^{(n)} \end{bmatrix} = 2\pi \int_0^{\pi} \mathrm{d}\theta\, \sin\theta\, P_n(\cos\theta) \begin{bmatrix} w_{k,k'} \\ e_{k,k'} \end{bmatrix}(\cos\theta). \tag{25}$$

Consequently, using the addition theorem for Legendre polynomials,

$$P_n(\hat{\boldsymbol{\omega}}' \cdot \hat{\boldsymbol{n}}) = \frac{4\pi}{2n+1} \sum_{p=-n}^{n} Y_{n,p}^*(\hat{\boldsymbol{\omega}}'|\hat{\boldsymbol{\omega}}) Y_{n,p}(\hat{\boldsymbol{n}}|\hat{\boldsymbol{\omega}}), \tag{26}$$

where $Y_{n,p}(\hat{\boldsymbol{\alpha}}|\hat{\boldsymbol{\omega}})$ is a spherical harmonic in a frame where $\hat{\boldsymbol{\omega}}$ defines the z-axis, we find that both $w_{k,k'}$ and $e_{k,k'}$ acting as integration kernels map P_n onto P_n,

$$\int \mathrm{d}\hat{\boldsymbol{\omega}}' \begin{bmatrix} w_{k,k'} \\ e_{k,k'} \end{bmatrix} (\hat{\boldsymbol{\omega}} \cdot \hat{\boldsymbol{\omega}}') P_n(\hat{\boldsymbol{\omega}}' \cdot \hat{\boldsymbol{n}}) = \begin{bmatrix} w^{(n)}_{k,k'} \\ e^{(n)}_{k,k'} \end{bmatrix} P_n(\hat{\boldsymbol{\omega}} \cdot \hat{\boldsymbol{n}}), \tag{27}$$

i.e. the P_n are eigenfunctions of $w_{k,k'}$ and $e_{k,k'}$. Turning back to equation (22), we can now conclude that therefore P_n are also eigenfunctions of this integral equation, and hence $f^{(1)}_m(\hat{\boldsymbol{\omega}}_m) = c_m P_n(\hat{\boldsymbol{\omega}}_m \cdot \hat{\boldsymbol{n}})$ for some $\hat{\boldsymbol{n}}$. The amplitudes c_m, which we will call the *degree of order* at the bifurcation, measure the relative strength of the ordering tendency of the given segment with respect to the other segments. They are defined up to a multiplicative constant.

We can now solve equation (22) by combining the above results in a step-by-step fashion. First we consider the infinitesimal effective field,

$$\sum_{k'} \int \mathrm{d}\hat{\boldsymbol{\omega}}' \, e_{k,k'}(\hat{\boldsymbol{\omega}}_k \cdot \hat{\boldsymbol{\omega}}') f^{(1)}_{k'}(\hat{\boldsymbol{\omega}}') = P_n(\hat{\boldsymbol{\omega}}_k \cdot \hat{n}) \sum_{k'} e^{(n)}_{k,k'} c_{k'}. \tag{28}$$

Next, we carry out an integration over the Boltzmann flexibility weight (suppose that $(j,k) \in \mathcal{P}_{k,m}$),

$$\int \mathrm{d}\hat{\boldsymbol{\omega}}_j \, \frac{w_{j,k}(\hat{\boldsymbol{\omega}}_j \cdot \hat{\boldsymbol{\omega}}_k)}{w^{(0)}_{j,k}} \sum_{k'} \int \mathrm{d}\hat{\boldsymbol{\omega}}' \, e_{k,k'}(\hat{\boldsymbol{\omega}}_k, \hat{\boldsymbol{\omega}}') f^{(1)}_{k'}(\hat{\boldsymbol{\omega}}') = P_n(\hat{\boldsymbol{\omega}}_j \cdot \hat{n}) \frac{w^{(n)}_{j,k}}{w^{(0)}_{j,k}} \sum_{k'} e^{(n)}_{k,k'} c_{k'}. \tag{29}$$

This process continues until segment m is reached and in every integration a factor $w^{(n)}_{j,j'}/w^{(0)}_{j,j'}$ (with $(j,j') \in \mathcal{P}_{k,m}$) is being picked up. All remaining Boltzmann flexibility integrations (with $(j,j') \notin \mathcal{P}_{k,m}$) simply yield $w^{(0)}_{j,j'}/w^{(0)}_{j,j'} = 1$. Consequently,

$$\begin{aligned} \int \prod_{j \neq m} \mathrm{d}\hat{\boldsymbol{\omega}}_j \prod_{j,j'}^{(j,j')} \frac{w_{j,j'}(\hat{\boldsymbol{\omega}}_j \cdot \hat{\boldsymbol{\omega}}_{j'})}{w^{(0)}_{j,j'}} \sum_{k'} \int \mathrm{d}\hat{\boldsymbol{\omega}}' \, e_{k,k'}(\hat{\boldsymbol{\omega}}_k \cdot \hat{\boldsymbol{\omega}}') f^{(1)}_{k'}(\hat{\boldsymbol{\omega}}') \\ = P_n(\hat{\boldsymbol{\omega}}_m \cdot \hat{n}) \left(\prod_{(j,j') \in \mathcal{P}_{k,m}} \frac{w^{(n)}_{j,j'}}{w^{(0)}_{j,j'}} \right) \sum_{k'} e^{(n)}_{k,k'} c_{k'}. \end{aligned} \tag{30}$$

Finally, combining this with equation (22) yields

$$c_m = -\frac{\rho}{4\pi} \sum_k \left(\prod_{(j,j') \in \mathcal{P}_{k,m}} \frac{w^{(n)}_{j,j'}}{w^{(0)}_{j,j'}} \right) \sum_{k'} e^{(n)}_{k,k'} c_{k'}, \tag{31}$$

where we have dropped the $P_n(\hat{\boldsymbol{\omega}}_m \cdot \hat{n})$ on both sides. Defining for notational purposes

$$W^{(n)}_{m,k} = \prod_{(j,j') \in \mathcal{P}_{k,m}} \frac{w^{(n)}_{j,j'}}{w^{(0)}_{j,j'}} \tag{32}$$

we are left with the following set of linear equations:

$$c_m = -\frac{\rho}{4\pi} \sum_k W^{(n)}_{m,k} \sum_{k'} e^{(n)}_{k,k'} c_{k'}. \tag{33}$$

Note that the linearity again shows that the normalization of the c_m can be freely chosen. The solution to equation (33) poses a diagonalization problem involving $M \times M$ matrices, which would appear to be hard for any reasonably sized chain. Fortunately, there is additional structure to this equation which allows a reduction to an $R \times R$-dimensional problem, where R is the number of different *types* of segments in the chain. As this number is typically limited, we get a significant reduction in complexity. This is the topic of the following section.

2.2.2. Bifurcation analysis at the type level. So far, the ODFs have been formulated for every segment separately. However, often we are more interested in the average ODF of a certain component, e.g. in the case of the main-chain LC polymers considered in the next part the average mesogen ODF or the average spacer ODF. Therefore, we define the average ODF of a certain type of segment in the following way:

$$f_\tau(\hat{\boldsymbol{\omega}}) = \frac{1}{M_\tau}\sum_{k\in\tau} f_k(\hat{\boldsymbol{\omega}}), \tag{34}$$

where M_τ is the number of segments of type τ in the whole chain. The sum in equation (34) is over all segments of type τ.

Next, we use the fact that $e_{k,k'}(\hat{\boldsymbol{\omega}}\cdot\hat{\boldsymbol{\omega}}') = e_{\tau,\tau'}(\hat{\boldsymbol{\omega}}\cdot\hat{\boldsymbol{\omega}}')$ with $k\in\tau$ and $k'\in\tau'$, so

$$\begin{aligned}\sum_{k'} e^{(n)}_{k,k'}c_{k'} &= \frac{1}{M_\tau}\sum_{\tau'} M_\tau M_{\tau'} e^{(n)}_{\tau,\tau'}\frac{1}{M_{\tau'}}\sum_{k'\in\tau'} c_{k'}\\ &= \frac{1}{M_\tau}\sum_{\tau'} M_\tau M_{\tau'} e^{(n)}_{\tau,\tau'}c_{\tau'}\end{aligned} \tag{35}$$

which defines c_τ. We also define two type dependent matrices

$$E^{(n)}_{\tau,\tau'} = M_\tau M_{\tau'} e^{(n)}_{\tau,\tau'} \tag{36}$$

$$W^{(n)}_{\tau,\tau'} = \frac{1}{M_\tau M_{\tau'}}\sum_{k\in\tau}\sum_{k'\in\tau'} W^{(n)}_{k,k'}, \tag{37}$$

corresponding to the excluded volume and flexibility contributions respectively. With these matrices, we can rewrite the eigenvalue equation (33) solely in terms of type dependent quantities,

$$c_\tau = -\frac{\rho}{4\pi}\sum_{\tau'} W^{(n)}_{\tau,\tau'}\sum_{\tau''} E^{(n)}_{\tau',\tau''}c_{\tau''}, \tag{38}$$

or in a convenient vector notation

$$\mathbf{c} = -\frac{\rho}{4\pi}\mathbf{W}^{(n)}\mathbf{E}^{(n)}\mathbf{c} \tag{39}$$

which is an $R\times R$-dimensional matrix equation. Note that $\mathbf{E}^{(n)}$ is simple to determine on the basis of the segment–segment excluded volumes, but that $\mathbf{W}^{(n)}$ explicitly depends on the structure of the whole polymer and its calculation is generally more involved.

We can label the real eigenvalues λ_i of $\mathbf{W}^{(n)}\mathbf{E}^{(n)}$ in such a way that $\lambda_1^{(n)}\leqslant\lambda_2^{(n)}\leqslant\lambda_3^{(n)}\ldots$. The physically relevant bifurcation is the one with the lowest value of the density. Denoting this density by ρ_* we find

$$\rho_* = -\frac{4\pi}{\min_n\lambda_1^{(n)}} = -\frac{4\pi}{\lambda_1^{(2)}}, \tag{40}$$

where we assume, as is verified *a posteriori* as in practically all cases, that $\lambda_1^{(n)}$ will be most negative for $n=2$.[3] The corresponding eigenvector $\mathbf{c}_*$ yields the order distribution (over the R different types) of the degree of order at the bifurcation and we usually normalize it by setting one of its components, for a given type τ, to unity (which means the degree of order of the remaining types is measured in units of that of τ).

In some cases, when there are competing ordering tendencies, it may be not trivial to determine the appropriate sign of $\mathbf{c}_*$, as both $+\mathbf{c}_*$ and $-\mathbf{c}_*$ are eigenvectors. It can be found

[3] If a mode different from $n=2$ drives the spinodal, there should be a distinct physical cause. An example is found in [48], where an isotropic fluid of so-called Onsager crosses becomes unstable with respect to a cubatic $n=4$ perturbation, compatible with the cubic symmetry of the particles.

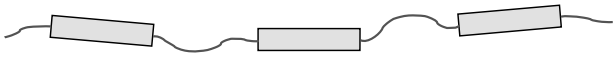

Figure 2. A few units of a main-chain LC polymer.

by considering the components of the vector $\mathbf{E}^{(2)}\mathbf{c}$, which must necessarily be positive to be consistent with the positive alignment of the components of the polymer, i.e. the strongest mesogens, that are driving the transitions. Such an ambiguous situation can for instance occur in the case of side-chain LC polymers with mesogens in the backbone as well as in the side-chains in the presence of bond angle constraints between the backbone and the spacers. However, in this case, one should in principle also check for the existence of biaxial nematic phases. This can be done by considering the second order of ε in the bifurcation analysis [45, 49].

So far, we have obtained the bifurcation density ρ_* as well as the distribution of the degree of order over the various types at bifurcation $c_{\tau_p,*}$. However, a final step in our programme is still possible, which allows us to obtain distribution of the degree of order $c_{m,*}$ at the bifurcation over all individual segments separately. This step requires a partial 'type' average, instead of a full one as in equation (37), of the matrix $W^{(2)}_{m,k}$

$$W^{(2)}_{m,\tau} \equiv \frac{1}{M_\tau} \sum_{k\in\tau} W^{(2)}_{m,k}. \tag{41}$$

When we combine this with equation (33), we obtain

$$c_{m,*} = -\frac{\rho_*}{4\pi} \sum_{\tau} W^{(2)}_{m,\tau} \sum_{\tau'} E^{(2)}_{\tau,\tau'} c_{\tau',*}. \tag{42}$$

Thus the the type order distribution $c_{\tau,*}$ determined in the previous step can be used to compute the order distribution $c_{m,*}$ by using equation (42). The calculation of the $M \times R$-matrix, which involves the evaluation of otherwise simple products along all paths from segments of a given to type to the target segment, is readily performed in the case of regular polymer topologies, as we will illustrate in the next part of this paper, where we perform this calculation for main-chain LC polymers.

3. Main-chain LC polymers

3.1. Introduction

A generic main-chain LC polymers consists of rigid mesogens connected via more flexible spacers in a linear fashion as depicted in figure 2. The mesogens provide the driving force for the LC phase transitions, whereas the spacers act to decouple the mesogens from each other. Still, the stiffness and the dimensions of the spacers can be of considerable influence on the location of the phase transition. Also, in an LC phase some degree of ordering will necessarily be imposed onto the spacers through the orientational interactions with the mesogens as well as other spacers. To fully unravel these various aspects, we will therefore study the simplest realization of a main-chain LC polymer, composed of just two types of segments, using the formalism and the solution tool, i.e. bifurcation analysis, developed in section 2. Although, initially, we describe the spacers as consisting of segmented chains, it is actually more convenient to treat them in the so-called 'wormlike chain limit'. We also consider the case where the polymer becomes infinite in length, making contact with previous mean-field approaches that have neglected end-effects. The results include the dependence of the I–N bifurcation density on the model parameters and profiles of the incipient order along

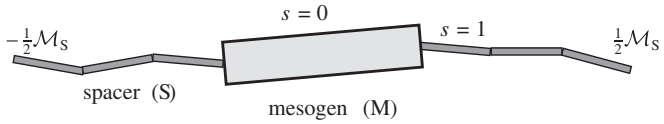

Figure 3. A unit of a main-chain LC polymer.

the chain at the bifurcation. We conclude with a comparison to previous work by Yurasova and co-workers [22–24] and Wang and Warner [25].

3.2. Model

3.2.1. Model parameters. Our simple model of a main-chain LC polymer consists of $\mathcal{N}$ repeating units, each containing a single ($\mathcal{M}_M = 1$) rigid mesogen (M) and $\mathcal{M}_S$ spacer (S) segments (see figure 3). Hence, $R = 2$ and we set $\tau_1 = S$ and $\tau_2 = M$. The mesogens have dimensions l_M and d_M and their total number in the polymer is $M_M = \mathcal{N}\mathcal{M}_M = \mathcal{N}$. The spacer segments have dimensions l_S and d_S and the number of spacer segments in one unit is $\mathcal{M}_S$, so the total number in the polymer is $M_S = \mathcal{N}\mathcal{M}_S$. Suppose for simplicity that $\mathcal{M}_S$ is even, so every unit consists of $\frac{1}{2}\mathcal{M}_S$ spacer segments, a mesogen segment and again $\frac{1}{2}\mathcal{M}_S$ spacer segments as depicted in figure 3. The segment label is m (or k) and runs along the chain; $m \in \{1, \ldots, M\}$, with $M = \mathcal{N}(\mathcal{M}_S + 1)$ the total number of segments. Every $(n(\mathcal{M}_S + 1) - \frac{1}{2}\mathcal{M}_S)$th segment (with $n \in \{1, \ldots, \mathcal{N}\}$ the label of a unit) is a mesogen; all the others are spacer segments. Often, we also use the relative label s within a unit, so then $m = n(\mathcal{M}_S + 1) - \frac{1}{2}\mathcal{M}_S + s$, where $s \in \{-\frac{1}{2}\mathcal{M}_S, \ldots, \frac{1}{2}\mathcal{M}_S\}$.

We now turn to the interactions. Between nearest-neighbour segments within a polymer, we use a generic bending potential which is locally harmonic in the bending angle around full mutual alignment,

$$u_{m,m+1}(\hat{\boldsymbol{\omega}} \cdot \hat{\boldsymbol{\omega}}') = -J_S \hat{\boldsymbol{\omega}} \cdot \hat{\boldsymbol{\omega}}'. \tag{43}$$

We assume this potential between all the spacer segments, but for simplicity also between the spacer and the mesogen segments. This avoids the introduction of an additional model parameter, at a small cost in generality. Finally, we recall the excluded volume between two segments m and m' on different polymers

$$e_{m,m'}(\hat{\boldsymbol{\omega}} \cdot \hat{\boldsymbol{\omega}}') = l_\tau l_{\tau'}(d_\tau + d_{\tau'})|\sin\gamma(\hat{\boldsymbol{\omega}} \cdot \hat{\boldsymbol{\omega}}')|, \tag{44}$$

where $m \in \tau$ and $m' \in \tau'$.

3.2.2. Wormlike chains and infinite polymers. Following the seminal work of Khokhlov and Semenov [14], the wormlike chain concept has been popular as a model for main-chain LC polymers. Indeed, wormlike chains are conceptually simpler than segmented chains with explicit bending potentials. We can transform our segmented chains into wormlike chains by applying the so-called wormlike chain limit (WCL, discussed in more detail [34]). However, as we want to keep the details of the differentiated molecular components in the case of the main-chain LC polymers, we only apply the WCL to the spacers, and take the limits

$$l_S \to 0, \qquad \beta J_S \to \infty, \qquad \mathcal{M}_S \to \infty, \tag{45}$$

while keeping the following combinations of parameters constant:

$$P_S = \beta J_S l_S \qquad \bar{\mathcal{M}}_S = \mathcal{M}_S/\beta J_S. \tag{46}$$

Here P_S is the persistence length of the spacers and $\bar{\mathcal{M}}_S$ the length of the spacer with a single repeat unit measured in units of the persistence [50]. The spacer segment labels become continuous as well, $\bar{m} = (m/M)\bar{M}$ and $\bar{s} = (s/\mathcal{M}_S)\bar{\mathcal{M}}_S$ (and therefore $m, s \to \infty$). In general, an overbar on a quantity refers to its appropriate value in the WCL. Apart from the conceptual simplification, the WCL also reduces the number of model parameters by one; $l_S, \beta J_S, \mathcal{M}_S \to P_S, \bar{\mathcal{M}}_S$. The WCL can be also be applied straightforwardly on the level of the bifurcation analysis (again, see [34]).

Typically, real main-chain LC polymers are very long (10^2–10^3 repeat units). Therefore it can also be interesting to consider the polymer to be infinitely long. In this case, due to translational symmetry along the chain, every unit is the same as its neighbour (and there are no free end effects). We call this limit the infinite polymer limit (IPL),

$$\mathcal{N} \to \infty, \qquad \rho \to 0 \qquad \text{with } \rho\mathcal{N} \text{ finite}, \tag{47}$$

where the polymer number density needs to be rescaled as well, as it is the mesogen density $\rho\mathcal{N}$ which drives the I–N transition. In this limit we lose yet another model parameter ($\mathcal{N}$).

Finally, we are free to adopt relative measures for the relevant lengths. As the dimensions of the mesogens are not subject to either the WCL or the IPL, they are the most logical choice to use as a reference. We therefore introduce the dimensionless spacer persistence length and spacer segment thickness as

$$\tilde{P}_S = P_S/l_M \qquad \text{and} \qquad \tilde{d}_S = d_S/d_M, \tag{48}$$

and define the following dimensionless density:

$$\eta = 2l_M^2 d_M \rho\mathcal{N}. \tag{49}$$

The result is that, after applying the WCL to the spacers, the finite-length main-chain LC polymers we have introduced here are described by only four model parameters, $\mathcal{M}_S$, $\tilde{P}_S$, $\tilde{d}_S$ and $\mathcal{N}$. If we consider infinitely long polymers, the dependence on $\mathcal{N}$ also drops out. In most physical situations, $\tilde{d}_S$ is significantly smaller than one. In fact, we will frequently consider the case $\tilde{d}_S = 0$. This is an instructive limiting case, because while there are no contributions from the SS interactions (there is no excluded volume between two zero-thickness spacers) the MS excluded volume is not zero, so these zero-thickness spacers still contribute to spacer–mesogen orientational coupling (equation (44)).

3.3. Bifurcation analysis

3.3.1. Bifurcation density. In this section we evaluate the elements of the matrices $\mathbf{E}^{(2)}$ and $\mathbf{W}^{(2)}$, which are needed to solve the type-averaged bifurcation equation, equation (39). We start by considering segmented chains, and apply the WCL and the IPL at a later stage.

Considering first the excluded volume part, we obtain from equations (6) and (36)

$$E^{(2)}_{\tau,\tau'} = s_2\mathcal{N}^2\mathcal{M}_\tau l_\tau \mathcal{M}_{\tau'} l_{\tau'}(d_\tau + d_{\tau'}), \tag{50}$$

where $\tau, \tau' \in \{S, M\}$ and $s_2 = -\pi^2/8$ is the second Legendre coefficient of $|\sin\gamma|$. We normalize $\mathbf{E}^{(2)}$ with respect to its lower right element $E^{(2)}_{MM}$, setting $\boldsymbol{\kappa} = (s_2\mathcal{N}^2 2l_M^2 d_M)^{-1}\mathbf{E}^{(2)}$. Then taking the WCL, $\boldsymbol{\kappa} \to \bar{\boldsymbol{\kappa}}$, we get

$$\bar{\boldsymbol{\kappa}} = \begin{bmatrix} \bar{\mathcal{M}}_S^2 \tilde{P}_S^2 \tilde{d}_S & \bar{\mathcal{M}}_S \tilde{P}_S \frac{1}{2}(1+\tilde{d}_S) \\ \bar{\mathcal{M}}_S \tilde{P}_S \frac{1}{2}(1+\tilde{d}_S) & 1 \end{bmatrix}. \tag{51}$$

We note that there is no $\mathcal{N}$-dependence in $\bar{\boldsymbol{\kappa}}$.

Next, we calculate the elements of the 2×2-matrix $\mathbf{W}^{(2)}$. There are two simplifying observations which can be made for this system: (i) all bending potentials are the same

(equation (43)) and then so are all the Boltzmann weights $w^{(2)}_{j,j'} = w^{(2)}$; (ii) the path $\mathcal{P}_{k,m}$ from segment k to segment m can be formulated in terms of a simple sequence of increasing numbers, i.e. $\mathcal{P}_{k,m} = \{(k, k+1), (k+1, k+2), \ldots, (m-1, m)\}$ (for $k < m$ and $\mathcal{P}_{k,m} = \mathcal{P}_{m,k}$). Consequently,

$$W^{(2)}_{m,k} = \prod_{(j,j')\in\mathcal{P}_{k,m}} \frac{w^{(2)}_{j,j'}}{w^{(0)}_{j,j'}} = \left(\frac{w^{(2)}}{w^{(0)}}\right)^{|k-m|} = \sigma^{|k-m|}, \tag{52}$$

which defines σ. Therefore, we get, according to equation (37),

$$W^{(2)}_{\tau,\tau'} = \frac{1}{M_\tau M_{\tau'}} \sum_{k\in\tau} \sum_{k'\in\tau'} \sigma^{|k-k'|}. \tag{53}$$

Next, we define $\boldsymbol{\alpha} = \mathcal{N}\mathbf{W}^{(2)}$, in order to have a more compact notation, but also because the rescaling with $\mathcal{N}$ is necessary in the IPL where the elements of $\mathbf{W}^{(2)}$ diverge. The expressions for the elements of $\boldsymbol{\alpha}$ are

$$\alpha_{\mathrm{S,S}} = \frac{\mathcal{N}}{\mathcal{N}^2\mathcal{M}_\mathrm{S}^2} \sum_{m,m'=1}^{\mathcal{N}(\mathcal{M}_\mathrm{S}+1)} \sigma^{|m-m'|} - \frac{\alpha_{\mathrm{S,M}} + \alpha_{\mathrm{M,S}}}{\mathcal{M}_\mathrm{S}} - \frac{\alpha_{\mathrm{M,M}}}{\mathcal{M}_\mathrm{S}^2} \tag{54}$$

$$\alpha_{\mathrm{S,M}} = \alpha_{\mathrm{M,S}} = \frac{\mathcal{N}}{\mathcal{N}^2\mathcal{M}_\mathrm{S}} \sum_{m=1}^{\mathcal{N}(\mathcal{M}_\mathrm{S}+1)} \sum_{n=1}^{\mathcal{N}} \sigma^{|m-(n(\mathcal{M}_\mathrm{S}+1)-\frac{1}{2}\mathcal{M}_\mathrm{S})|} - \frac{\alpha_{\mathrm{M,M}}}{\mathcal{M}_\mathrm{S}} \tag{55}$$

$$\alpha_{\mathrm{M,M}} = \frac{\mathcal{N}}{\mathcal{N}^2} \sum_{n,n'=1}^{\mathcal{N}} \sigma^{|n-n'|(\mathcal{M}_\mathrm{S}+1)} \tag{56}$$

where we have (partly) expressed the elements in a recursive fashion. We note that all sums above can be performed analytically. However, as we are mainly interested in the results in the WCL for the spacers, we do not perform these computations here. In the WCL, σ becomes (to first order in $1/\beta J_\mathrm{S}$)

$$\sigma = \frac{\int_{-1}^{1} \mathrm{d}x\ P_2(x) \exp[\beta J_\mathrm{S} x]}{\int_{-1}^{1} \mathrm{d}x\ \exp[\beta J_\mathrm{S} x]} \to 1 - 3(\beta J_\mathrm{S})^{-1}, \tag{57}$$

and therefore

$$\sigma^{\mathcal{M}_\mathrm{S}} \to \left(1 - 3(\beta J)^{-1}\right)^{\beta J \bar{\mathcal{M}}_\mathrm{S}} = \exp\left[-3\bar{\mathcal{M}}_\mathrm{S}\right], \tag{58}$$

where we have used $\lim_{n\to\infty}(1 + \frac{x}{n})^n = \mathrm{e}^x$. As an example, we evaluate the summation in equation (56) (over n and n'),

$$\frac{1}{\mathcal{N}} \sum_{n,n'=1}^{\mathcal{N}} \sigma^{|n-n'|(\mathcal{M}_\mathrm{S}+1)} \to \frac{1}{\mathcal{N}} \sum_{n,n'=1}^{\mathcal{N}} \mathrm{e}^{-3\bar{\mathcal{M}}_\mathrm{S}|n-n'|} = \frac{1 + \mathrm{e}^{-3\bar{\mathcal{M}}_\mathrm{S}}}{1 - \mathrm{e}^{-3\bar{\mathcal{M}}_\mathrm{S}}} \left(1 - \frac{2\mathrm{e}^{-3\bar{\mathcal{M}}_\mathrm{S}}}{\mathcal{N}} \frac{1 - \mathrm{e}^{-3\mathcal{N}\bar{\mathcal{M}}_\mathrm{S}}}{1 - \mathrm{e}^{-6\bar{\mathcal{M}}_\mathrm{S}}}\right). \tag{59}$$

For the summations over m, we note that these become integrals in the WCL,

$$\frac{1}{\mathcal{N}\mathcal{M}_\mathrm{S}} \sum_{m=1}^{\mathcal{N}(\mathcal{M}_\mathrm{S}+1)} \to \frac{1}{\mathcal{N}\bar{\mathcal{M}}_\mathrm{S}} \int_0^{\mathcal{N}\bar{\mathcal{M}}_\mathrm{S}} \mathrm{d}\bar{m}, \tag{60}$$

and finally, the contributions due to $\alpha_{\mathrm{M,M}}$ in equation (55) and those due to $\alpha_{\mathrm{M,M}}$ and $\alpha_{\mathrm{S,M}}$ in equation (54) go to zero in WCL. Skipping the details of the evaluation of the remaining

integrals, we immediately move on to the results, and equations (54)–(56) become, in the WCL, $\boldsymbol{\alpha} \to \bar{\boldsymbol{\alpha}}$,

$$\bar{\alpha}_{\mathrm{S,S}} = \frac{2}{3\bar{\mathcal{M}}_{\mathrm{S}}}\left(1 - \frac{1 - \mathrm{e}^{-3\mathcal{N}\bar{\mathcal{M}}_{\mathrm{S}}}}{3\mathcal{N}\bar{\mathcal{M}}_{\mathrm{S}}}\right) \tag{61}$$

$$\bar{\alpha}_{\mathrm{S,M}} = \bar{\alpha}_{\mathrm{M,S}} = \frac{2}{3\bar{\mathcal{M}}_{\mathrm{S}}}\left(1 - \frac{\mathrm{e}^{-\frac{3}{2}\bar{\mathcal{M}}_{\mathrm{S}}}}{\mathcal{N}}\frac{1 - \mathrm{e}^{-3\mathcal{N}\bar{\mathcal{M}}_{\mathrm{S}}}}{1 - \mathrm{e}^{-3\bar{\mathcal{M}}_{\mathrm{S}}}}\right) \tag{62}$$

$$\bar{\alpha}_{\mathrm{M,M}} = \frac{1 + \mathrm{e}^{-3\bar{\mathcal{M}}_{\mathrm{S}}}}{1 - \mathrm{e}^{-3\bar{\mathcal{M}}_{\mathrm{S}}}}\left(1 - \frac{2\mathrm{e}^{-3\bar{\mathcal{M}}_{\mathrm{S}}}}{\mathcal{N}}\frac{1 - \mathrm{e}^{-3\mathcal{N}\bar{\mathcal{M}}_{\mathrm{S}}}}{1 - \mathrm{e}^{-6\bar{\mathcal{M}}_{\mathrm{S}}}}\right). \tag{63}$$

Taking the IPL is trivial, given the explicit dependence on $\mathcal{N}$, and the matrix $\bar{\boldsymbol{\alpha}}$ reduces to very simple form in this limit,

$$\bar{\boldsymbol{\alpha}} = \begin{bmatrix} \frac{2}{3\bar{\mathcal{M}}_{\mathrm{S}}} & \frac{2}{3\bar{\mathcal{M}}_{\mathrm{S}}} \\ \frac{2}{3\bar{\mathcal{M}}_{\mathrm{S}}} & \frac{1+\mathrm{e}^{-3\bar{\mathcal{M}}_{\mathrm{S}}}}{1-\mathrm{e}^{-3\bar{\mathcal{M}}_{\mathrm{S}}}} \end{bmatrix}. \tag{64}$$

We now collect the results and reformulate the bifurcation equation, equation (39), in terms of the newly defined $\bar{\boldsymbol{\kappa}}$, $\bar{\boldsymbol{\alpha}}$, η. In the WCL, $\mathbf{c} \to \bar{\mathbf{c}}$, it becomes

$$\bar{\mathbf{c}} = -\frac{\eta s_2}{4\pi}\bar{\boldsymbol{\alpha}}\bar{\boldsymbol{\kappa}}\bar{\mathbf{c}}. \tag{65}$$

As the problem is two dimensional, it has solutions

$$-\frac{\eta s_2}{4\pi} = \frac{\pi\eta}{32} = 2\Big/\left(\mathrm{tr}(\bar{\boldsymbol{\alpha}}\bar{\boldsymbol{\kappa}}) \pm \sqrt{\mathrm{tr}^2(\bar{\boldsymbol{\alpha}}\bar{\boldsymbol{\kappa}}) - 4\det(\bar{\boldsymbol{\alpha}}\bar{\boldsymbol{\kappa}})}\right), \tag{66}$$

with 'tr' and 'det' being the trace and determinant of matrices respectively. $\mathrm{tr}(\bar{\boldsymbol{\alpha}}\bar{\boldsymbol{\kappa}})$ is always larger than zero and $\det(\bar{\boldsymbol{\alpha}}\bar{\boldsymbol{\kappa}})$ can be both positive and negative. Furthermore, it can be checked as well that $\mathrm{tr}^2(\bar{\boldsymbol{\alpha}}\bar{\boldsymbol{\kappa}}) \geqslant 4\det(\bar{\boldsymbol{\alpha}}\bar{\boldsymbol{\kappa}})$ for this system, so that the eigenvalues are real. Consequently, the physical bifurcation density is given by

$$\eta_* = \frac{64}{\pi}\Big/\left(\mathrm{tr}(\bar{\boldsymbol{\alpha}}\bar{\boldsymbol{\kappa}}) + \sqrt{\mathrm{tr}^2(\bar{\boldsymbol{\alpha}}\bar{\boldsymbol{\kappa}}) - 4\det(\bar{\boldsymbol{\alpha}}\bar{\boldsymbol{\kappa}})}\right), \tag{67}$$

and, putting the mesogen order to one, $\bar{\mathbf{c}}_* = \left(\bar{c}_{\mathrm{S},*}, 1\right)$, we get for the average order of the spacers,

$$\bar{c}_{\mathrm{S},*} = (2(\bar{\boldsymbol{\alpha}}\bar{\boldsymbol{\kappa}})^{(2,1)})^{-1}\left((\bar{\boldsymbol{\alpha}}\bar{\boldsymbol{\kappa}})^{(1,1)} - (\bar{\boldsymbol{\alpha}}\bar{\boldsymbol{\kappa}})^{(2,2)} + \sqrt{\mathrm{tr}^2(\bar{\boldsymbol{\alpha}}\bar{\boldsymbol{\kappa}}) - 4\det(\bar{\boldsymbol{\alpha}}\bar{\boldsymbol{\kappa}})}\right), \tag{68}$$

with $(\bar{\boldsymbol{\alpha}}\bar{\boldsymbol{\kappa}})^{(i,j)}$ being the (i, j)th element of the matrix $\bar{\boldsymbol{\alpha}}\bar{\boldsymbol{\kappa}}$.

As a check, but also to make contact with previous work, we mention a few limiting cases of our system for which the results at the level of the bifurcation analysis are known. In the case of zero-length spacers (by putting $\tilde{P}_{\mathrm{S}} = 0$), the polymers reduce to chains of mesogens, coupled via zero-size hinges and coupling constants $\exp(-3\bar{\mathcal{M}}_{\mathrm{S}})$. For this system, the bifurcation density is given by equation (65) in [34], in which $\sigma = \exp(-3\bar{\mathcal{M}}_{\mathrm{S}})$. Another case is obtained when $\bar{\mathcal{M}}_{\mathrm{S}} = 0$, and the polymers reduce to long stiff rods of length $\mathcal{N}l_{\mathrm{M}}$, i.e. the original Onsager model. For this system, the bifurcation density was calculated by Kayser and Raveché, $\eta_*\mathcal{N} = 32/\pi$ in [46]. The last limiting case is a bit less accessible. The result for a homogeneous wormlike chain can be obtained by taking the limit where $P_{\mathrm{S}} \gg l_{\mathrm{M}}$, or $l_{\mathrm{M}} \to 0$ (so the mesogens disappear). This means that we have to rescale the density η in terms of P_{S} instead of l_{M}. In this way, we reobtain the results for this case which are given in [14, 34].

3.3.2. Degree of order along the polymer. The degree of order of the individual segments along the polymer at the bifurcation point can be calculated using equations (41) and (42). To this end we first define the (primed) matrix $\alpha'_{m,\tau'} = \mathcal{N} W^{(2)}_{m,\tau'}$. In the WCL, the discrete segment label m becomes continuous and the $M \times 2$-matrix $\boldsymbol{\alpha}'$ reduces to a set of 2×2-matrices $\bar{\boldsymbol{\alpha}}'$: $\alpha'_{m,\tau'} \to \bar{\alpha}'_{\tau,\tau'}(\bar{m})$, where $\bar{m} \in \tau$. However, the difference between $\bar{\alpha}_{\tau,\tau'}$ and $\bar{\alpha}'_{\tau,\tau'}(\bar{m})$ is that the latter still depends on the label $\bar{m} \in \tau$ and as a consequence is not symmetric in the type labels. The evaluation of the elements of $\bar{\boldsymbol{\alpha}}'$ is similar to that of $\bar{\boldsymbol{\alpha}}$, so we give them without further comment,

$$\bar{\alpha}'_{\mathrm{S,S}}(\bar{s}, n) = \frac{1}{3\bar{\mathcal{M}}_{\mathrm{S}}} \left(2 - \mathrm{e}^{-3(\bar{s}+(n-\frac{1}{2})\bar{\mathcal{M}}_{\mathrm{S}})} - \mathrm{e}^{-3((\mathcal{N}-n+\frac{1}{2})\bar{\mathcal{M}}_{\mathrm{S}}-\bar{s})} \right) \tag{69}$$

$$\bar{\alpha}'_{\mathrm{S,M}}(\bar{s}, n) = \mathrm{e}^{-3|\bar{s}|} + \mathrm{e}^{-3(\bar{\mathcal{M}}_{\mathrm{S}}+\bar{s})} \frac{1 - \mathrm{e}^{-3(n-1)\bar{\mathcal{M}}_{\mathrm{S}}}}{1 - \mathrm{e}^{-3\bar{\mathcal{M}}_{\mathrm{S}}}} + \mathrm{e}^{-3(\bar{\mathcal{M}}_{\mathrm{S}}-\bar{s})} \frac{1 - \mathrm{e}^{-3(\mathcal{N}-n)\bar{\mathcal{M}}_{\mathrm{S}}}}{1 - \mathrm{e}^{-3\bar{\mathcal{M}}_{\mathrm{S}}}} \tag{70}$$

$$\bar{\alpha}'_{\mathrm{M,S}}(n) = \frac{1}{3\bar{\mathcal{M}}_{\mathrm{S}}} \left(2 - \mathrm{e}^{-3(n-\frac{1}{2})\bar{\mathcal{M}}_{\mathrm{S}}} - \mathrm{e}^{-3(\mathcal{N}-n+\frac{1}{2})\bar{\mathcal{M}}_{\mathrm{S}}} \right) \tag{71}$$

$$\bar{\alpha}'_{\mathrm{M,M}}(n) = \frac{1 + \mathrm{e}^{-3\bar{\mathcal{M}}_{\mathrm{S}}} - \mathrm{e}^{-3n\bar{\mathcal{M}}_{\mathrm{S}}} - \mathrm{e}^{-3(\mathcal{N}-n+1)\bar{\mathcal{M}}_{\mathrm{S}}}}{1 - \mathrm{e}^{-3\bar{\mathcal{M}}_{\mathrm{S}}}}, \tag{72}$$

where we have used $\bar{m} = (n, \bar{s})$ with $n \in \{1 \ldots \mathcal{N}\}$ the unit dependence and $\bar{s} \in [-\frac{1}{2}\bar{\mathcal{M}}_{\mathrm{S}}, \frac{1}{2}\bar{\mathcal{M}}_{\mathrm{S}}]$ runs within a unit. In the case of infinite polymer length, both $\mathcal{N}$ and n (and their difference, $\mathcal{N} - n$) become infinite, and one readily sees which terms in equations (69)–(72) drop out. In all cases the following relation holds:

$$\bar{\boldsymbol{\alpha}} = \frac{1}{\mathcal{N}\bar{\mathcal{M}}_{\mathrm{S}}} \sum_{n=1}^{\mathcal{N}} \int_{-\frac{1}{2}\bar{\mathcal{M}}_{\mathrm{S}}}^{\frac{1}{2}\bar{\mathcal{M}}_{\mathrm{S}}} \mathrm{d}\bar{s}\, \bar{\boldsymbol{\alpha}}'(\bar{s}, n). \tag{73}$$

So, having solved the eigenvalue problem, equation (65), for η_* and $\bar{\mathbf{c}}_*$, one can compute the order along the polymer with

$$\bar{\mathbf{c}}'_* = \begin{pmatrix} \bar{c}'_{\mathrm{S},*}(\bar{s}, n) \\ \bar{c}'_{\mathrm{M},*}(n) \end{pmatrix} = -\frac{\eta_* s_2}{4\pi} \bar{\boldsymbol{\alpha}}'(\bar{s}, n) \bar{\boldsymbol{\kappa}} \bar{\mathbf{c}}_*, \tag{74}$$

where the normalization is again chosen such that the average mesogen order equals unity, $(1/\mathcal{N}) \sum_{n=1}^{\mathcal{N}} \bar{c}'_{\mathrm{M},*}(n) = 1$.

3.4. Results

Having set up our formalism in the previous section, we are now in a position to present results on the bifurcation density and the order along the polymer as a function of model parameters. We first of all vary the spacer length, $\bar{\mathcal{M}}_{\mathrm{S}}$, as this is experimentally an accessible parameter. We also look at the effect of increasing chain length, $\mathcal{N}$, or equivalently the degree of polymerization. The degree of order along the polymer at the bifurcation is plotted as well, both for infinitely long chains (where we plot just one unit) and for finite lengths. The remaining parameters are, unless stated otherwise, chosen to be $\tilde{P}_{\mathrm{S}} = 0.3$ and $\tilde{d}_{\mathrm{S}} = 0$. Our aim is not so much to be exhaustive, but rather to bring out the salient features of our approach.

In figure 4 the bifurcation density (left) and average spacer order (right) are plotted as a function of spacer length, $\bar{\mathcal{M}}_{\mathrm{S}}$. When $\bar{\mathcal{M}}_{\mathrm{S}} = 0$, the chain is exactly a sequence of $\mathcal{N}$ rigidly connected mesogens of length l_{M}, or equivalently one long mesogen of length $\mathcal{N} l_{\mathrm{M}}$. Consequently, $\eta_*(\bar{\mathcal{M}}_{\mathrm{S}} = 0) = 32/\pi\mathcal{N}$ and $\bar{c}_{\mathrm{S},*}(\bar{\mathcal{M}}_{\mathrm{S}} = 0) = 1$. Increasing $\bar{\mathcal{M}}_{\mathrm{S}}$, the mesogens become more decoupled from each other, and the bifurcation density goes up. (Except for $\mathcal{N} = 1$, as in this case there is only one mesogen per molecule. Here increasing the spacer length is equivalent to increasing the dimensions of the molecule and as a result the

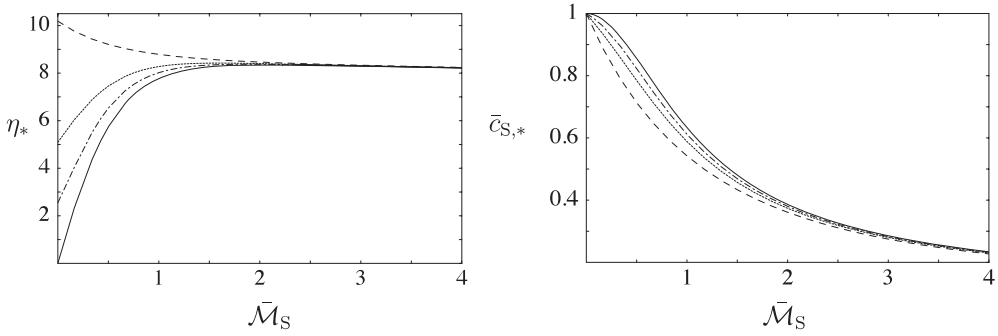

Figure 4. The I–N bifurcation density (left) and the degree of order of the spacers at the bifurcation (right) as a function of spacer length, $\bar{\mathcal{M}}_S$, for various values of the polymer length, $\mathcal{N}$. The parameters are $\tilde{P}_S = 0.3$ and $\tilde{d}_S = 0$. The values for the polymer lengths are $\mathcal{N} = 1$ (dashed line), $\mathcal{N} = 2$ (dotted line), $\mathcal{N} = 4$ (dash–dotted line) and $\mathcal{N} = \infty$ (solid line). It can be checked that at $\bar{\mathcal{M}}_S = 0$, $\eta_* = 32/\pi\mathcal{N}$ (the rigid rod result). The average order of the mesogens is set equal to unity.

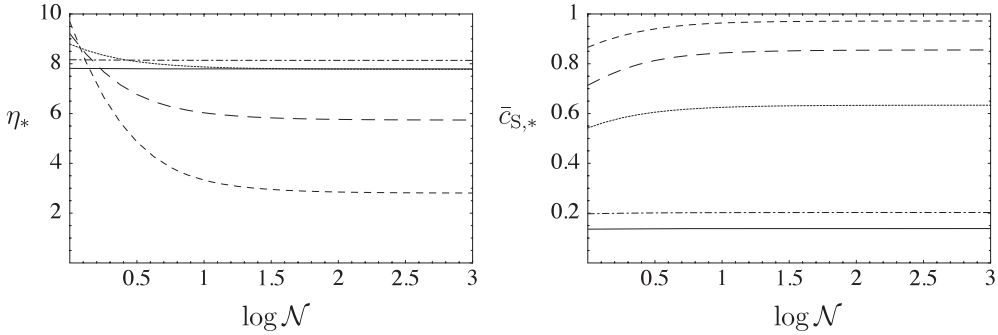

Figure 5. The dependence of the bifurcation density (left) and the degree of order of the spacers at the bifurcation (right) on the length of the polymer for various spacer lengths. The parameters are $\tilde{P}_S = 0.3$, $\tilde{d}_S = 0$. The spacer lengths are $\bar{\mathcal{M}}_S = 0.2$ (dashed line), $\bar{\mathcal{M}}_S = 0.5$ (long dashed line), $\bar{\mathcal{M}}_S = 1$ (dotted line), $\bar{\mathcal{M}}_S = 5$ (dash–dotted line) and $\bar{\mathcal{M}}_S = 10$ (solid line).

bifurcation density goes down.) When the dimensionless spacer length roughly exceeds three, the mesogens are totally decoupled. Going to even larger spacer lengths only increases the overall dimensions of the molecules and, therefore, η_* goes down slowly. This is hardly visible in figure 4, but this effect is more pronounced for $\tilde{d} \neq 0$. The average order (figure 4 (right)) of the spacers decreases with increasing $\bar{\mathcal{M}}_S$, as the mesogen concentration in the chain effectively gets diluted more and more and the resulting orientational ordering field on the spacers within the chain decreases.

In figure 5, the dependence of the bifurcation density (left) and the spacer order (right) on the length of the polymer is plotted for a range of values of $\bar{\mathcal{M}}_S$. For $\mathcal{N} = 1$ (so at $\log\mathcal{N} = 0$) there is only one mesogen, so the longer the spacer (=tails) the lower the bifurcation density. However, increasing $\mathcal{N}$ long spacers yield disconnected mesogens, whereas in the case of short spacers the mesogens are coupled more tightly. Consequently, the curves for short spacers drop to much lower values than for long spacers. However, as we mentioned before, when the spacer length exceeds a certain value the mesogens are already disconnected and longer spacers correspond to bigger molecules and thus a lower bifurcation density: therefore, the curve for $\bar{\mathcal{M}}_S = 10$ lies below that of $\bar{\mathcal{M}}_S = 5$ in figure 5 (left). In figure 5 (right), the spacer order

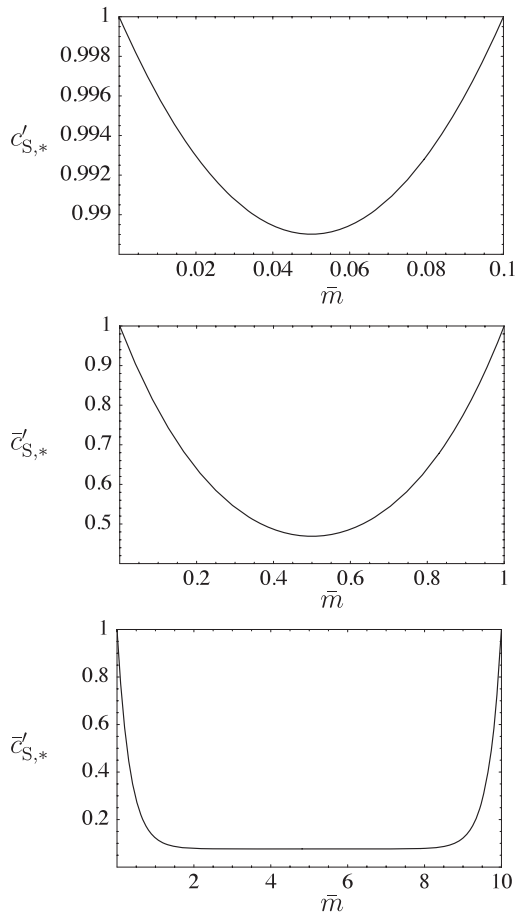

Figure 6. Order along the spacers for infinitely long polymers, $\mathcal{N} \to \infty$, and only one spacer is shown. The parameters are $\tilde{P}_S = 0.3$, $\tilde{d}_S = 0.$ and $\bar{\mathcal{M}}_S = 0.1$ (top), $\bar{\mathcal{M}}_S = 1$ (middle) and $\bar{\mathcal{M}}_S = 10$ (bottom). In this case, we use a label $\bar{s} \in [0, \bar{\mathcal{M}}_S]$, although this profile technically consists of two consecutive half units. The mesogens are located at $\bar{s} = 0$ and $\bar{\mathcal{M}}_S$ and have order equal to 1.

simply increases with $\mathcal{N}$ because the effect of the free (and necessarily less ordered) chain ends decreases. This effect is more pronounced for shorter spacer lengths which are already more ordered than longer spacers in the first place.

The order along infinitely long polymers is plotted in figure 6. The top (very short spacers) and bottom plots (very long spacers) are extreme cases; the middle plot is for spacers of intermediate lengths. Starting with the very long spacers, we see that the order of spacer right next to the mesogens (at $\bar{s} = 0$) is the same as the mesogen order (=1), but when moving away from the mesogens it 'relaxes' to a plateau. For intermediate lengths, the same happens, but now the relaxation tails seem to overlap, and a plateau region is no longer identified. For small lengths, the shape of the order profile is the same as for intermediate lengths but the scale of variation of the order is much smaller. In this case the spacers are basically forced to adopt the order imposed by the neighbouring mesogens.

Finally, in figure 7, we have plotted the order along a polymer with a finite number $\mathcal{N} = 13$ of repeat units. Three different spacer lengths have been considered and chosen such that they

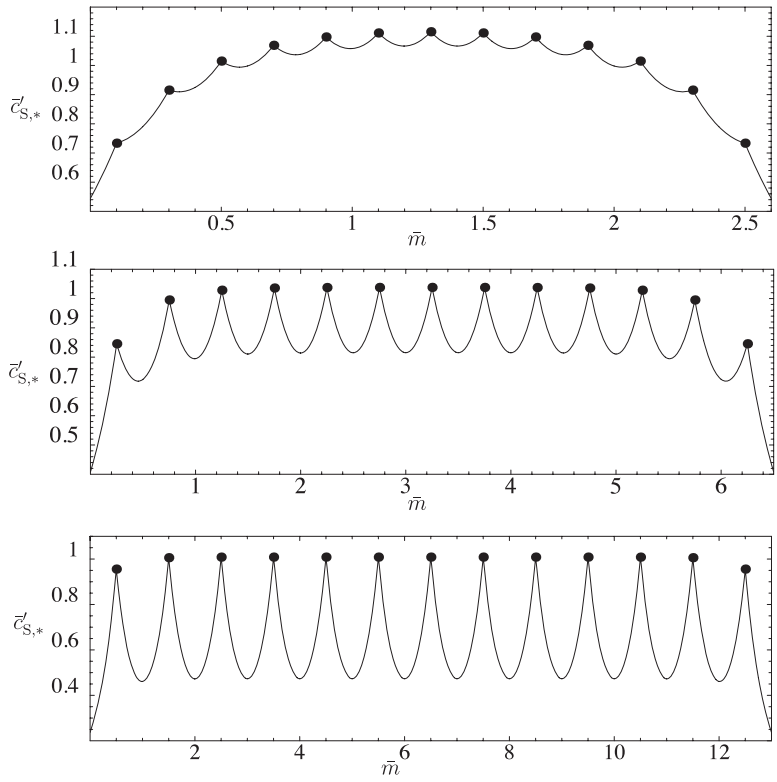

Figure 7. Order along the chain for a finite-length polymer, $\mathcal{N} = 13$. The black dots are the mesogens and the lines are the spacers. The parameters are $\tilde{P}_S = 0.3$, $\tilde{d}_S = 0$ and $\bar{\mathcal{M}}_S = 0.2$ (top), $\bar{\mathcal{M}}_S = 0.5$ (middle) and $\bar{\mathcal{M}}_S = 1$ (bottom). The label $\bar{m} \in [0, \mathcal{N}\bar{\mathcal{M}}_S]$, the mesogens (black dots) are located at $\bar{m} = (n - \frac{1}{2})\bar{\mathcal{M}}_S$ with $n \in \{1, \ldots, \mathcal{N}\}$ and the average order of the mesogens is unity.

illustrate the effect of the finite length of the polymer on the order profile. In general, for homogeneous linear LC polymers it is a well known result that in the nematic phase the order at the free ends is lower (by exactly a factor of two for infinitely long ones) than in the middle. In the case of the top plot, the spacers are quite short, and the influence of the free ends propagates out several units (about five or six) to the middle of the chain. As a result the spacers in between the mesogens are ordered almost equally strongly as the neighbouring mesogens themselves. In the middle and the bottom plot, the spacers are longer, and therefore the number of units that 'feel' the ends is smaller (two or three). Simultaneously, the spacers can adopt a more disordered conformation.

4. Conclusion and discussion

In section 2 we have developed a formalism for dealing with a very general class of liquid-crystalline polymers composed of rigid segments. The main virtues of the approach are its ability to deal, without any additional approximations, with branched molecular structures and compositional heterogeneity. Moreover, we show through a formal bifurcation analysis that many interesting properties relating to the ordering transition can be extracted from the theory in an analytical fashion. This is illustrated in section 3, where we treat a simple model for a

main-chain LC polymer, consisting of mesogenic blocks connected by more flexible spacers. The resultant theory has a limited number of parameters (three for infinitely long polymers or four for finite ones). Noteworthy results are (i) the dependence of the bifurcation density on the spacer length $\bar{\mathcal{M}}_S$, showing the steep increase for small values of this length, thus rationalizing the experimentally established fact that sufficiently long spacers are necessary to decouple the mesogens, (ii) perhaps the first calculations of the distribution of the degree of order along such structured chain molecules and (iii) a proof that N–N transitions are not possible for this system.

In order to compare our work to earlier approaches, we first turn to the work of Yurasova *et al* [22–24], which treats a similar molecular geometry, but now composed of segments interacting through a Maier–Saupe potential, and hence thermally driven. They use the so-called spherical approximation to analytically compute the free energy for infinitely long polymers, resulting in a theory with four parameters. The appearance of an additional parameter, compared to our model in the same case, is due to the fact that for an excluded volume interaction the dimensions of the two different segments fully fix the interactions (MM, MS and SS), whereas in the case of Maier–Saupe-like theories a separate energetic parameter has to be specified for each of the possible interactions. Their results on the dependence of the transition temperature on spacer length, with a minimum for a certain spacer length, flanked by a steep increase for smaller spacer lengths and a very shallow increase for larger spacer lengths, are very similar to ours (see figure 4 (left)), if one takes into account that the temperature translates into the *inverse* density in the mapping between the two formalisms. A somewhat unphysical result they obtain is that for large spacer lengths the order parameter at the phase transition of the spacers is larger than that of the mesogens, suggesting unrealistically that, in that case, the spacers are driving the transition. This artefact is probably due to the fact that their model effectively assigns an orientational interaction energy per unit length to the spacers that unless some form of scaling is applied will outstrip the contributions of the mesogens, that remain fixed in size. A similar approach was followed by Wang and Warner [25], who also use a Maier–Saupe type theory with four parameters to describe the same system of infinitely long polymers. They write down an exact, at least as far as the intra-molecular degrees of freedom are concerned, formulation of the partition function. This partition function is then expanded in terms of spheroidal wavefunctions, of which they keep only the 'ground state' contribution. In the resulting stationarity equations contributions do appear which are related to the fact that the components are embedded in a polymer. In a way, this is a first-order correction, with respect to the internal degrees of freedom of the polymer, to a pure decoupled Maier–Saupe type mean field theory. They do, however, report a strong decrease of transition temperature for small spacer lengths, which is consistent with the decrease of the bifurcation density shown in figure 4.

In the present work we have limited ourselves to a bifurcation analysis of the stationarity equation (12). In principle it is of course possible to solve them numerically, as we have done for linear homopolymers in [34] and side-chain polymers in [35]. The rationale for doing so however is slight. We have already shown in section 2 that there are no nematic-to-nematic phase transitions within the present theory (equation (20)). This is also consistent with the results of [22–25]. So far, N–N transitions for main-chain LC polymers have only been discussed for lattice models [18–20, 51]. We thus expect that the mesogens as well as the spacers only exhibit a smooth increase of ordering on an increase of the density in the nematic phase. Of course, an explicit numerical calculation would be required to obtain the coexistence densities, but experience shows that they are typically within a few per cent of the analytically determined bifurcation density. Consequently, we have not performed these numerical calculations for this system.

The model of a main-chain LC polymer is of course extremely simplified. There are several aspects that could be considered within the framework of our theory. One is compositional randomness, as occurs in copolymers in which neither the mesogens nor the spacers have constant lengths [1]. Such heterogeneity is readily incorporated within our theory. From a practical point of view, however, the interesting aspect of random copolymers is that they reduce the tendency to crystallize and enhance glassy behaviour. This effect lies far outside the scope of the present approach. Another issue is polydispersity; due to the way these main-chain LC polymers are synthesized they are inevitably polydisperse in chain lengths [1, 2, 6]. Polydispersity of this type can also easily be included in the present approach, but the effect of polydispersity in chain lengths is only expected to be significant for relatively short polymers. As a last issue we address the so-called odd–even effect. In many experimental systems [1, 2, 6], it is often observed that spacers consisting of an even number of CH_2 have significantly higher transition temperatures than those with an odd number of CH_2-groups. In order to model these effects we would need to consider next-nearest-neighbour interactions along the chain to include the different rotational-isomeric states. This is in principle possible, as our approach can be generalized to arbitrary finite ranged interactions along the chain, albeit at the cost of increased complexity.

Finally, spatially inhomogeneous (i.e. smectic) phases are extremely common for LC polymers [1, 2, 6]. Indeed, in principle one could check the stability of the isotropic phase with respect to smectic perturbations within our theory as well. However, the increase in complexity is enormous, as we now need to couple the molecular conformation to spatial density wave, which varies significantly (one expects the dominant wavelength to be comparable to the length of the mesogenic units) over the scale of the polymer as a whole. Nevertheless, the relevant driving mechanisms for inhomogeneous phases are present in this system of different-size hard anisotropic components; hard rods are able to form smectic phases [52] and it has e.g. been shown that binary mixtures of thick and thin hard rods tend to demix already in the isotropic phase due to (relatively) unfavourable interactions between the thick and thin rods [53, 54]. Purely entropic interactions are thus expected to be sufficient to drive smectic phase formation, with its concomitant microscale demixing between spacers and mesogens, in LC polymers (see e.g. [55]). Therefore, the problem of solving the isotropic or nematic-to-smectic bifurcation equations, either analytically or numerically, remains an open challenge.

Acknowledgments

We thank one of the referees for drawing our attention to [33]. This work is part of the research programme of the Stichting voor Fundamenteel Onderzoek der Materie (FOM), which is financially supported by the Nederlandse organisatie voor Wetenschappelijk Onderzoek (NWO).

References

[1] Donald A and Windle A 1992 *Liquid Crystalline Polymers* (Cambridge: Cambridge University Press)
[2] Shibaev V P and Lam L (ed) 1994 *Liquid Crystalline and Mesomorphic Polymers* (Berlin: Springer)
[3] McArdle C B (ed) 1989 *Side Chain Liquid Crystalline Polymers* (Glasgow: Blackie)
[4] Ciferri A, Krigbaum W R and Meyer R B (ed) 1982 *Polymer Liquid Crystals* (New York: Academic)
[5] Platé N A and Shibaev V P 1987 *Comb-Shaped Polymers and Liquid Crystals* (New York: Plenum)
[6] Demus D, Goodby J, Gray G W, Spiess H-W and Hill V (ed) 1998 *Handbook of Liquid Crystals* vol 3 *High Molecular Weight Liquid Crystals* (New York: Wiley–VCH)
[7] Finkelmann H, Ringsdorf H and Wendorff J H 1978 *Makromol. Chem.* **179** 273
[8] Finkelmann H, Ringsdorf H, Siol W and Wendorff J H 1978 *Makromol. Chem.* **179** 829

[9] Finkelmann H, Happ M, Portugal M and Ringsdorf H 1978 *Makromol. Chem.* **179** 2541
[10] Onsager L 1949 *Ann. New York Acad. Sci.* **51** 627
[11] Flory P J 1956 *Proc. R. Soc.* A **234** 73
[12] Maier W and Saupe A 1959 *Z. Naturf.* **14** 882
[13] Khokhlov A R and Semenov A N 1981 *Physica* A **108** 546
[14] Khokhlov A R and Semenov A N 1982 *Physica* A **112** 605
[15] Warner M, Gunn J M F and Baumgärtner A B 1985 *J. Phys. A: Math. Gen.* **18** 3007
[16] Wang X J and Warner M 1986 *J. Phys. A: Math. Gen.* **19** 2215
[17] Matheson R R and Flory P J 1981 *Macromolecules* **14** 954
[18] Vasilenko S V, Shibaev V P and Khokhlov A R 1982 *Makromol. Chem., Rapid Commun.* **3** 917
[19] Vasilenko S V, Khokhlov A R and Shibaev V P 1984 *Macromolecules* **17** 2270
[20] Matsuyama A and Kato T 1998 *J. Chem. Phys.* **109** 2023
[21] Semenov A N and Vasilenko S V 1986 *Sov. Phys.—JETP* **63** 70
[22] Yurasova T A and Semenov A N 1990 *Polym. Sci.: USSR* **32** 223
[23] Yurasova T A and Semenov A N 1991 *Mol. Cryst. Liq. Cryst.* **199** 301
[24] Yurasova T A and McLeish T C B 1993 *Polymer* **34** 3774
[25] Wang X J and Warner M 1992 *Liq. Cryst.* **12** 385
[26] Vertogen G and van der Meer B W 1979 *Physica* A **99** 237
[27] Wilson M R and Allen M P 1993 *Mol. Phys.* **80** 277
[28] Dijkstra M and Frenkel D 1995 *Phys. Rev.* E **51** 51
[29] Lyulin A V, Al-Barzani M S, Allen M P, Wilson M R, Neelov I and Allsopp N K 1998 *Macromolecules* **31** 4626
[30] Ilnytskyi J and Wilson M R 2001 *Comput. Phys. Commun.* **134** 23
[31] Bhadradwaj R K and Boyd R H 1998 *Macromolecules* **31** 7682
[32] Pavel D, Ball J, Bhattacharya S, Shanks R, Hurduc N and Catanescu O 2001 *Comput. Theoret. Polym. Sci.* **11** 303
[33] Stott J J and Petschek R G 1999 *Liq. Cryst.* **26** 1393
[34] Wessels P P F and Mulder B M 2003 *Soft Mater.* **1** 313
[35] Wessels P P F and Mulder B M 2003 *Europhys. Lett.* **64** 337
[36] Wessels P P F and Mulder B M 2006 Isotropic-to-nematic transition in LC heteropolymers: II. Side chain LC polymers *J. Phys.: Condens. Matter* **18** 9359
[37] Evans R 1979 *Adv. Phys.* **28** 143–200
[38] Vroege G J and Lekkerkerker H N W 1992 *Rep. Prog. Phys.* **55** 1241
[39] Holyst R and Oswald P 2001 *Macromol. Theory Simul.* **10** 1
[40] Hansen J-P and McDonald I R 1986 *Theory of Simple Liquids* 2nd edn (New York: Academic)
[41] Morita T 1976 *Physica* A **83** 411
[42] Herzfeld J, Berger A E and Wingate J W 1984 *Macromolecules* **17** 1718
[43] Wang X and Warner M 1987 *J. Phys. A: Math. Gen.* **20** 713
[44] Renz W and Warner M 1988 *Proc. R. Soc. Lond.* A **417** 213
[45] Terzis A F, Vanakaras A G and Photinos D J 2000 *Mol. Cryst. Liq. Cryst.* **352** 265
[46] Kayser R F Jr and Raveché H J 1978 *Phys. Rev.* A **17** 2067
[47] Mulder B 1989 *Phys. Rev.* A **39** 360
[48] Blaak R and Mulder B M 1998 *Phys. Rev.* E **58** 5873
[49] Wessels P P F 2002 Flexible theories for flexible molecules *PhD Thesis* FOM Institute for Atomic and Molecular Physics (AMOLF) The thesis can be found in a digital form on www.amolf.nl. Printed copies can be obtained from the library of AMOLF, library@amolf.nl.
[50] Flory P J 1989 *Statistical Mechanics of Chain Molecules* (Munich: Hanser)
[51] Semenov A N and Khokhlov A R 1988 *Sov. Phys.—Usp.* **31** 988
[52] Mulder B M 1987 *Phys. Rev.* A **35** 3095
[53] Sear R P and Jackson G 1995 *J. Chem. Phys.* **103** 8684
[54] van Roij R and Mulder B M 1996 *Phys. Rev.* E **54** 6430
[55] Wessels P P F and Mulder B M 2004 *Phys. Rev.* E **70** 031503